Synthesis and Characterization of $CuMnO_x$-Bentonite as Efficient Catalyst for Oxidation of *m*-xylene

[1]Mo Thi Nguyen, [1]Cam Minh Le, [1]Tuan Minh Nguyen, [3]Hao Hoang Nguyen, [2]Anwar-ul-Haq Ali Shah
[1]Hung Van Hoang*
[1]*Department of Physical Chemistry, Hanoi National University of Education, 136 Xuan Thuy, Hanoi Veitnam.*
[2]*Institute of Chemical Sciences, University of Peshawar, 25120, Pakistan.*
[3]*Vinh University, Vinh City, Vietnam.*
hunghv@hnue.edu.vn*

(Received on 1st July 2019, accepted in revised form 5th March 2020)

Summary: Catalytic oxidation of organic volatile compounds (VOCs) is considered superior to conventional methods because very low concentration of VOCs can also be oxidized and removed at low temperatures without consumption of addditional fuel and introduction of NO_x compounds into the environment. Herein, the synthesis of MnO_2 nanoparticles on bentonite (Bent) support in the presence of CuO for catalytic oxidation of m-xylene is reported. The synthesized materials were analyzed with FT-IR, XRD, and TEM analysis for structural and morphological characterization. XRD and TEM analysis indicated the formation of δ-MnO_2 with sheet structure on Bent surface. Temperature-programmed reduction (H_2-TPR) of hydrogen was used to investigate catalytic performance of δ-MnO_2 towards oxidation of m-xylene at different temperatures. The catalytic activity was strongly dependent on the δ-MnO_2 content in the synthesized material. 100 % oxidation of m-xylene with observed with 10% Mn content at temperature below than 325 °C. Intersetingly introduction of CuO greatly improved the catalytic activity of Mn-Bent materials. The presence of Cu in Mn-Bent has greatly reduced the temperature for complete oxidation of m-xylene. In this case100% conversion of m-xylene was observed at 250 °C.

Keywords: VOCs, Catalyst, Oxidative process, Bentonite, MnO_2.

Introduction

Volatile organic compounds (VOCs) have been considered as the major contributors to air pollution. The VOCs can come from different sources including petroleum refineries, fuel conbustions, solvent processes, chemical and textile industries, cleaning products and several other processes. The effect of VOCs is influenced by their nature, concentration and emission sources. However, VOCs have been proven to be harmful to both human and animals owing to the toxic, mutagenic and carcinogenic characteristics, and also responsible for reduction of ozone layer at stratosphere, secondary aerosol and photochemical smog. Therefore, it is extremely needed to reduce the concentration of VOCs in the air. In recent years, various methods, including adsorption, biofiltration, thermal incineration and catalytic oxidation have been used for VOCs removal [1]. However, catalytic oxidation was found to be a great way to reduce VOCs. The advantage of this method is that the VOCs can be removed at low concentration and low temperature in comparison to some conventional methods, which require additional fuels and form NO_x compounds. In addition, the catalytic oxidation can remove VOCs with highly efficiency, be highly regenerated with stable performance. Supported metal catalysts are reported to show high catalytic activity for deep oxidation of VOCs at low temperature. However, their relatively high cost, poor stability, rapid deactivation by chlorinated compounds, sulfur or other metals, as well as sublimation and sinterization problems have hindered their further development and wide applications in industries [1-5]. Instead of using expensively noble metals, many transition metal oxides which are cheaper and easier to synthesize, such as oxides of Fe, Cr, Ni, Cu Ce and Mn, have been employed as catalysts for VOCs removal [6-10]. Among those transition metal oxides, CuO and MnO_x oxides are found to exhibit high activity in the catalytic oxidation of VOCs and are environmentally friendly materials [11-13]. However, the relatively low surface area and the aggregation of these oxides may limit oxidation efficiency of VOCs. In order to overcome this drawback, incorporated with a supported material is a good solution. Bentonite with a layered structure having high thermal stability and high adsorability has been considered as a supported material which has potential applications in pollution treatment.

In this study, CuO and MnO_x oxides have been synthesized on supporting bentonite as catalyst material for oxidation of m-xylene. The structure of

*To whom all correspondence should be addressed.

obtained materials was characterized using X-ray diffraction (XRD), Fourier tranform infrared spectorscopy (FT-IR) and Transmission electron microscopy (TEM). The catalytic performnce of the as synthesized materials towards m-xylene was also investigated with temperature-programmed reduction of hydrogen (H_2-TPR) method.

Experimental

Materials

All chemicals including $Mn(NO_3)_2$ (50 wt%) solution, $H_2C_2O_4.2H_2O$, NH_3 (28% wt) solution, solid $(NH_4)_2S_2O_8$, $KMnO_4$, $Cu(NO_3)_2.3H_2O$, NaOH and liquid $C_{17}H_{33}COOH$ were purchased from Sigma-Aldrich at analytical grade and used as received. Double distilled water was used to prepare all solutions. Bentonite was provided by Co Dinh, Vietnam.

Synthesis

MnO_x: Typically, 30 mL of the solution containing 0.41 g of $Mn(NO_3)_2$ obtained from 50% $Mn(NO_3)_2$ solution was added slowly to 30 mL of the solution containing 1.14 g of $KMnO_4$ under vigorous stirring condition. The obtained mixture was continuously tirred for 4 hours and transferred to autoclave and then heated at constant temperature (160^{o}C) for 12 hours. The solid MnO_x (denoted as MnO_x-permanganate) thus formed was separated by filtration, washed with double distilled water, dried and calcinced at 400^{o}C for 4 hours.

MnO_x supported bentonite material: Firstly, 2.0 g of bentonite was added to the 30 mL of the solution containing 0.22 g of $KMnO_4$ under vigorous stirring to form dispersed mixture. Then 30 mL of the solution containing 0.08 g of $Mn(NO_3)_2$ obtained from 50% $Mn(NO_3)_2$ solution was added slowly to the mixture with continuous stirring. After vigorous stirring at 80^{o}C for 48 hours, the mixture was filtered, washed and dried at 50 ^{o}C for 24 hours. The obtained solid material was finally calcined at 400^{o}C for 4 hours and denoted as 5Mn-Bent (5 is mass percent of Mn in the sample).

The synthesis was carried out with different contents of Mn. The obtained materials were denoted as XMn-Bent (X = 10, 15 and 20).

MnO_x-CuO mixture supported bentonite material: Initially, 2.0 g of bentonite was added to the 30 mL of the solution containing 0.43 g of $KMnO_4$ with strong stirring. Then 30 mL of the solution containing 0.165 g of $Mn(NO_3)_2$ obtained from 50% $Mn(NO_3)_2$ solution and 0.012 g of $Cu(NO_3)_2$ was added dropwise to above mixture with strong stirring at 80^{o}C. After vigorous stirring for 48 hours, the mixture was filtered, washed and dried at 50^{o}C for 24 hours. The solid filtrate was finally calcined at 400 ^{o}C for 4 hours and denoted as 0.2Cu10Mn-Bent (0.2 and 10 are mass percent of Cu and Mn in the sample, respectively).

The synthesis was repeated with different contents of Cu. The obtained materials were denoted as VCuXMn-Bent (V = 0.1 and 0.5, X= 10).

Characterization

X-ray diffraction (XRD) patterns of the synthesized samples were recorded with a Bruker-D5005 powder X-ray diffractometer using Cu Kα-radiation with λ = 1.5406 Å. Fourier transform infrared spectroscopy (FT-IR) was performed on NEXUS-670, Nicotet – USA. The information on the particle size and morphology was provided by transmission electron microscopic (TEM) analysis. TEM images of the samples were acquired on a JEOL JEM-2010 microscope with an accelerating voltage of 200 kV. Elemental composition of the sanples was analyzed using energy-dispersive X-ray spectroscopy (EDX) with JEOL SM-6510LV microscope. Temperature programmed reduction (TPR) experiments were performed in an Autochem II 2920, Automated Catalyst Characterization System (Micromeritics). In all TPR experiments, the temperature was started from ambient temperature to desired temperature at a heating rate of 10 ^{o}C min^{-1}. Hydrogen gas (H_2) was used as reducing gas. Copper (II) oxide was used to calibrate the equipment. Quantitative calculation for TPR experiments was assumed that MnO is the final product of the MnO_x reduction at the end of the experiments.

Catalytic activity of samples was tested using a U-shaped quartz continuous flow reactor, employing catalysts samples of 0.30 g at atmospheric pressure. Before testing, the catalysts were treated at 400 ^{o}C in N_2-O_2 mixture (with the ratio of 4:1), and then cooled down to the reaction temperature in the same stream. Heating was supplied by an electrical furnace equipped with a temperature controller and

the reaction temperature was measured using a K-type thermocouple placed alongside but external to the catalyst bed. The reactant was fed to the reactor by a flow of O_2 + N_2 passing through a container filled with *m*-xylene, which was kept at 0 ^oC by immersing the *m*-xylene container in an ice/water bath. A flow of *m*-xylene in N_2/O_2 mixture had been allowed through the catalyst with a *m*-xylene/O_2 ratio equal to 1/100 and the total gas flow rate of 2L h^{-1}. A fraction of the influent and effluent gas stream was analyzed by a Shimadzu gas chromatograph (type GC-14A) equipped with FID-detector. The oxidation reaction of *m*-xylene has been investigated in the range of 150 ^oC − 325^oC with a step of 25^oC.

Results and Discussion

Bentonite and Mn-Bentonite

XRD patterns of bentonite and Mn-Bentonite

It has been reported that MnO_2, especially MnO_2 existing in the form of nano particles, prepared from manganese acetate and potassium permanganate has a good catalytic activity. Over *nano*-MnO_2, *m*-xylene can be oxidized completely at relatively low temperature (under 240 ^oC). However, the powder form of MnO_2 produces difficulties in practical applications. Therefore, scattering MnO_2 on supporting materials, which exists in the large size or can be easy to make seed-form, is a new trend to fabricate the catalysts for oxidation of VOCs in industry. In order to improve the catalytic activity of MnO_2, we have distributed MnO_2 on supporting bentonite with different contents of Mn.

The XRD patterns of pristine bentonite and MnO_2-bentonite samples with different contents of Mn are shown in Fig 1. The XRD pattern of bentonite, with peaks characteristic for quartz appearing with low density, reveals that bentonite is relatively pure with the main content of montmorillonite. While, peaks at 2θ: 12.2^o; 25.0^o and 37.5^o characteristic for birnessite δ-MnO_2 were seen in the XRD patterns of Mn-Bent samples [14]. Intensity of these peaks increases wit the increase of Mn content from 5% to 10%. However, when Mn content increases from 10% to 20%, the intensity of thes peaks remain nearly unchange. Wang *et al.* [15] proved that δ-MnO_2 was intermediate product in the formation of nanotubes of α-MnO_2 and β-MnO_2. In our study, α-MnO_2 was obtained from the reaction between manganese acetate and potassium permanganate; however, δ-MnO_2 was formed in the same procedure in the presence of bentonite. This may be due to the formation of MnO_2 on the surface of bentonite hindering the transformation from layered δ-MnO_2 to nanotube α-MnO_2

FT-IR spectra of Mn-Bent samples

Fig. 2 shows FT-IR spectra of synthesized bent and Mn-Bent samples in the range of 400 to 800 cm^{-1}. The absorption bands in all samples (bentonite with and without MnO_2) are similar; appearing around 459, 521 and 671 cm^{-1}. The similarlity of the FT-IR spectra of the the samples indicates that the introduction of MnO_2 on the bentonite surface can not be clearly identified from FT-IR spectra. Nevertheless, the presence of MnO_2 on the bentonite surface inceases the sharpness of the absorption band at 459 cm^{-1} and 521cm^{-1} characteristic for Mn-O vibration in octahedron of δ-MnO_2 [16]. This result is in good agreement with result obtainted from XRD analysis which has proved the formation of δ-MnO_2 on bentonite surface.

TEM images of Mn-Bent samples

The surface morphology of catalysts is an important factor, which affects to catalytic activity of the materials. In order to see the difference in morphology of the bentonite-Mn samples with different Mn contents, the synthesized materials were examined with TEM analysis. Fig 3 displays TEM images of Mn-Bent materials. Wang *et al.* [15] have reported that δ-MnO_2 alone has a layer structure, while other forms of MnO_2 exist in the tubular or wire or rod structures. It is appearent in the Fig 3 that MnO_2 formed on bentonite surface exists in the form of sheets similar to δ-MnO_2. However, at low content of Mn (5%) the MnO_2 scaterred on the bentonite like dots ununiformly with the size ranging from 50 nm to 300 nm. The number of dots appears more in the TEM images of the samples with higher Mn loading. At the Mn loading of 15% and 20%, MnO_2 sheets cover almost the entire surface of bentonite.

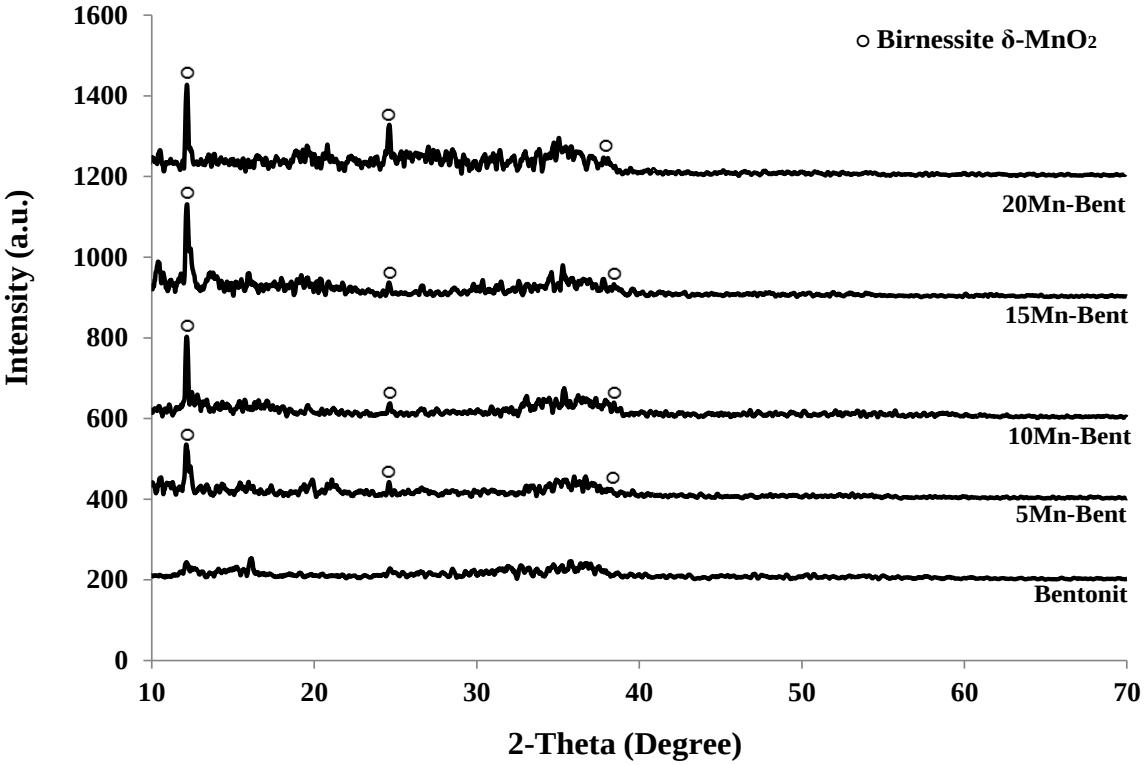

Fig. 1: XRD patterns of bentonite and Bentonite-MnO_2 with different contents of Mn as indicated.

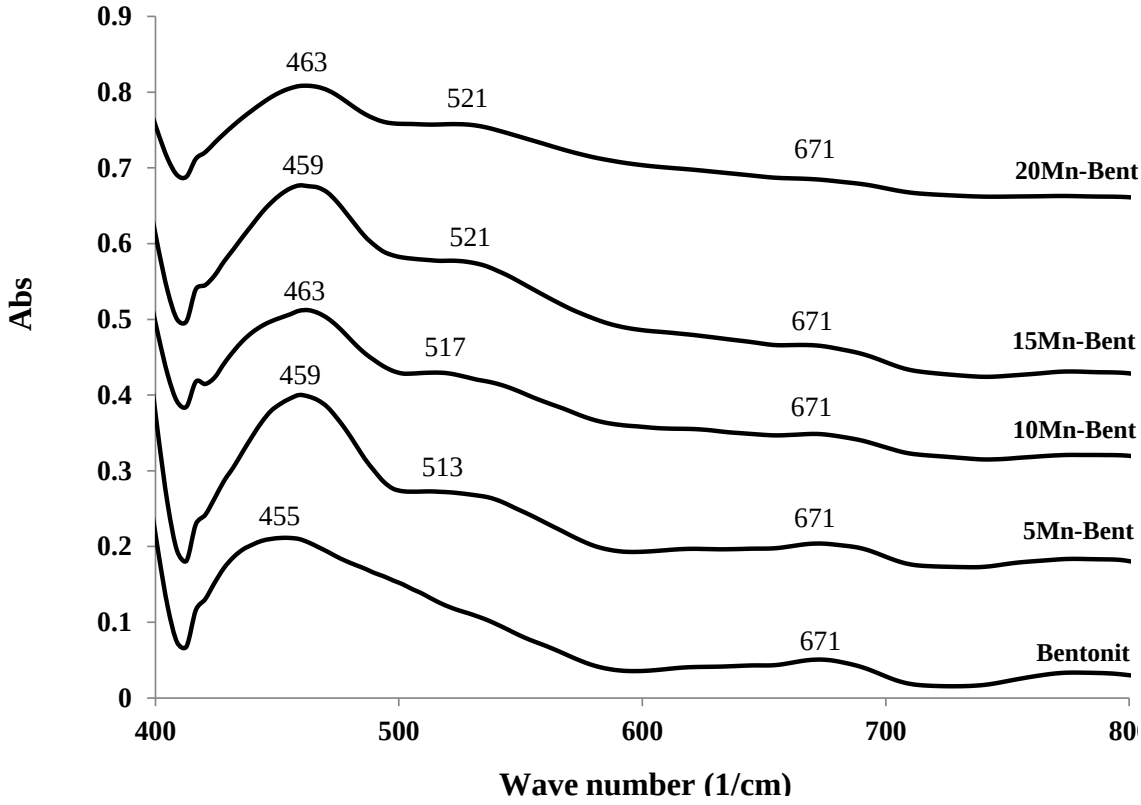

Fig. 2: FT-IR spectra of Mn-Bent samples with different Mn contents.

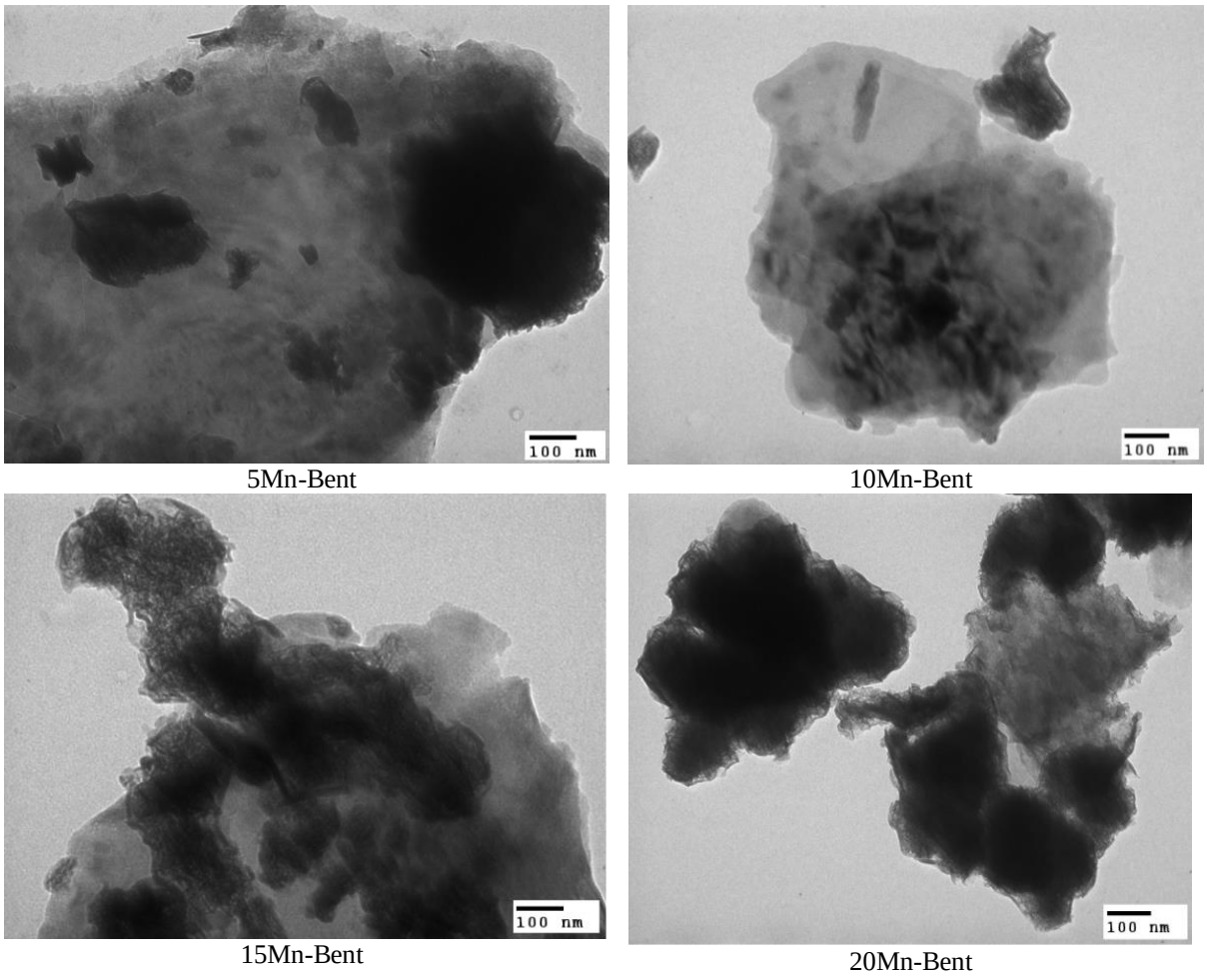

Fig. 3: TEM images of Bentonite and Mn-Bent with different Mn contents.

Catalytic activity of Mn-Bent samples

The reducibility of XMn-Bent sapmles was studied by H_2-TPR measurement. Fig. 4 shows H_2-TPR profiles of MnO_x and 10Mn- Bent samples. The reduction of MnO_2 has been proved to happen through stages: $MnO_2 \rightarrow Mn_2O_3 \rightarrow Mn_3O_4 \rightarrow MnO$. It is evident from the three peaks in Fig. 4a for H_2-TPR profile of MnO_x, that H_2 consumption was observed at 192 ^oC, 241^oC and 285^oC corresponding to different reduction stages from MnO_2 to MnO. However, these peaks are not so clear due to the overlapping shoulder peaks of reduction peaks. This observation can be explained due to the simultaneous formation of MnO and intermediate substances Mn_2O_3 and Mn_3O_4 during the reduction of MnO_2 [17], and proves that MnO_x is very reactive and reduced at lower temperature than 300^oC.

For 10Mn-Bent, five peaks at 257.5 ^oC, 282.4 ^oC, 332.0^oC, 453.1^oC and 625.6^oC can be seen in the H_2-TPR profile, in which two peaks at the temperature less than 300^oC were assigned to the reduction of MnO_x on surface of bentonite. The reduction peak at 332.0 ^oC is due to the reduction of MnO_2 or Mn_2O_3 to Mn_3O_4 and the peak at 453.1^oC is related to the reduction of Mn_3O_4 to MnO. Besides, there is a broad peak at 625.6 ^oC in the H_2-TPR profile of 10Mn-Bent. This peak was assigned to the reduction of Mn^{3+} to Mn^{2+} occurring in the MnO_x incorporated to surface of supporting material [18]. As shown in Table-1, it is obvious that the content of Mn in 10Mn-Bent is just 10%, therefore, the total amount of consumed hydrogen (3.22 mmol g^{-1}) in the case of 10Mn-Bent is much smaller than the total consumed hydrogen (8.83 mmol g^{-1}) in the case of MnO_x-permanganate.

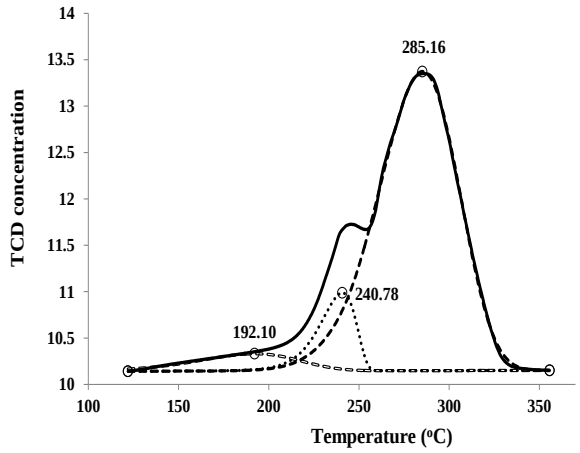

(a)

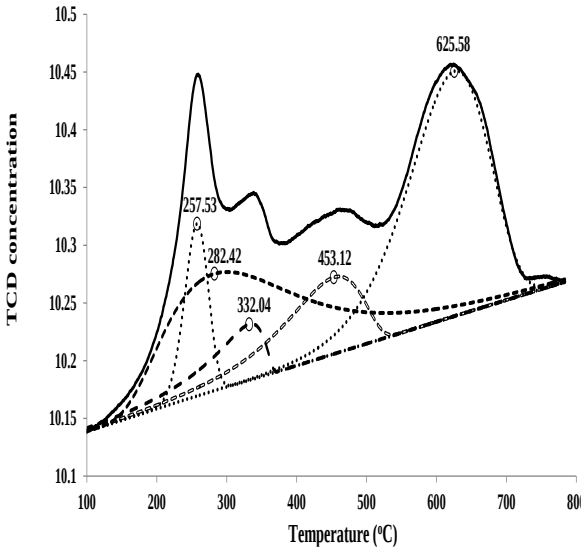

(b)

Fig. 4: H_2-TPR profiles of (a) MnO_x and (b) 10Mn-Bent.

Table-1: Amount of hydrogen consumed by MnO_x and 10Mn- Bent.

MnO_x-pemanganat	
Temperature of reduction peak [°C]	**Consumed H_2 [mmol g^{-1}]**
192.1	**0.55**
240.8	**0.90**
285.2	**7.38**
Total	**8.83**

10Mn-Bent	
Temperature of reduction peak [°C]	**Consumed H_2 [mmol g^{-1}]**
257.5 °C	**0.26 mmol/g**
282.4	**1.05**
332.0	**0.21**
453.1	**0.41**
625.6	**1.29**
Total	**3.22**

Catalytic activity of MnO_x-Bent samples on the oxidative reaction of m-xylene

The catalytic activity of MnO_x–Bent samples with different Mn contents ranging from 5 to 20 % was studied on the oxidation of m-xylene. The obtained results are presented in Fig. 5. Obviously, the catalytic activity increases relatively significant as the Mn content increases from 5 to 10%. However, when the Mn content exceeds beyond 10%, the catalytic activity decreases slightly. This decrease of catalytic activity may be due to the aggregation of MnO_x particles producing thick layer and therefore covering surface of supporting material and reducing catalytic activity of materials. 10Mn-Bent (with 10% Mn contentment) performed the highest catalytic activity in comparison to other samples with the conversion of 50% at 208 °C and 100% at the temperature under 325 °C. As displayed Fig. 4, though the catalytic activity of 10Mn-Bent is relatively high, it is still significantly lower than the catalytic activity of pure MnO_x.

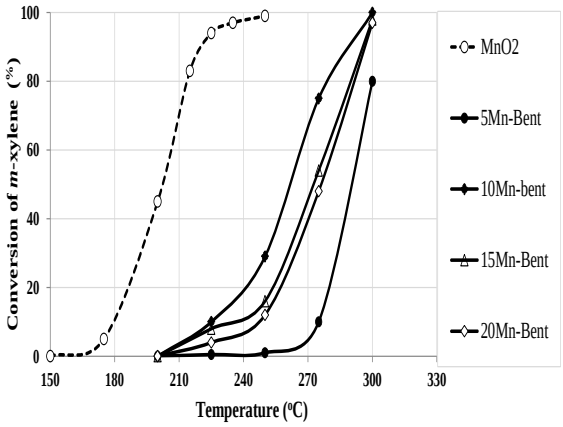

Fig. 5: Catalytic activity of MnO_x –Bent with different Mn contents in the oxidation of m-xylene.

CuO-MnO_x- Bent materials

In order to improve the catalytic performance of Mn-Bent materials, CuO was additionally introduced into 10Mn-Bent material with different contents of CuO (0.2, 0.5 and 1.0%) denoted as 0.2Cu10Mn-Bent; 0.5Cu10Mn-Bent và 1.0Cu10Mn-Bent, respectively.

XRD anylysis of CuMn-Bent

Fig. 6 depicts XRD patterns of the synthesized CuMn-Bent samples with the constant

Mn content of 10% and Cu content of 0.0, 0.1, 0.5 and 1.0%. As depicted in the XRD patterns, characteristic peaks of δ-MnO_2 were observed for all samples. However, intensity of these peaks decreases with the increase of Cu content. This may be explained due to the presence of Cu in the sample influencing the formation of δ-MnO_2. In all samples, no characteristic of CuO was obsevered. The content of Cu in samples is relatively low ranging from 0.1 to 1.0%. This may be the main reason leading to the absence of characteristic peaks of CuO in all samples.

Morphology of CuMn-Bent samples

Fig. 7 displays TEM images of CuMn-Bent samples with different Cu contents. As can be seen, thin sheets of MnO_x are still formed and cover uniformly on bentonite surface with the presence of CuO, although there is no observation of CuO in the TEM images. The presence of CuO in samples produces the uniform distribution of MnO_x on supporting surface.

EDX spectra of CuMn-Bent samples

The elemental analysis of CuMn-Bent samples confirms the presence of O, Si, Al, Fe and Mg as main components of bentonite (Table-2). The content of these elements varies insignificantly when MnO_2 and CuO are dispersed on the surface of bentonite. The Mn loading in CuMn-Bent is determined to be in the range of 8.99% ÷ 9.63%, which is closed to expected percentage of Mn in the synthesized samples (10%). The Cu loading in 10Mn-Bent; 0.2Cu10Mn-Bent; 0.5Cu10Mn-Bent and 1Cu10Mn-Bent are 0.17%; 0.35%; 0.68% and 1.32%, respectively. The Cu content is found to be approximate to the expected value with a minor excess probably due to the presence of a small amount of Cu in the orginial bentonite material. The EDX results indicate high effecciency of MnO_x and CuO loading on the bentonite material.

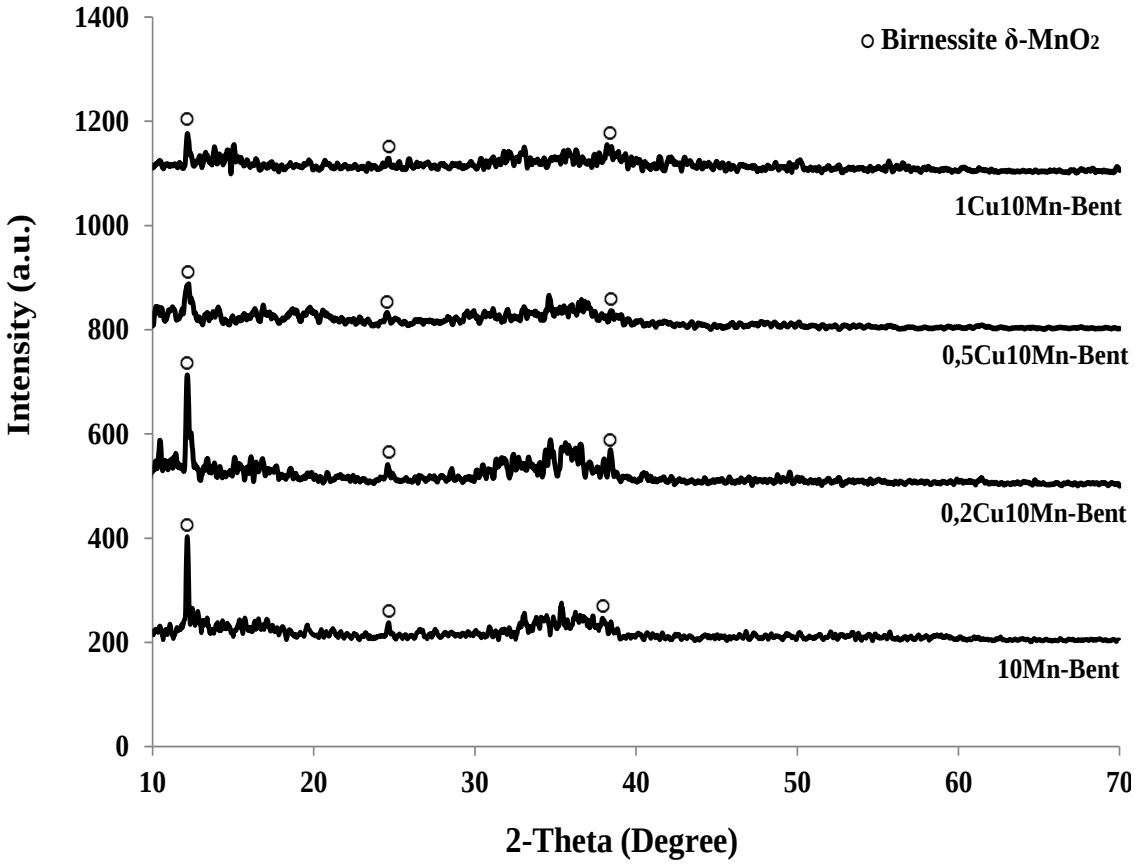

Fig. 6: XRD patterns of CuMn-Bent samples.

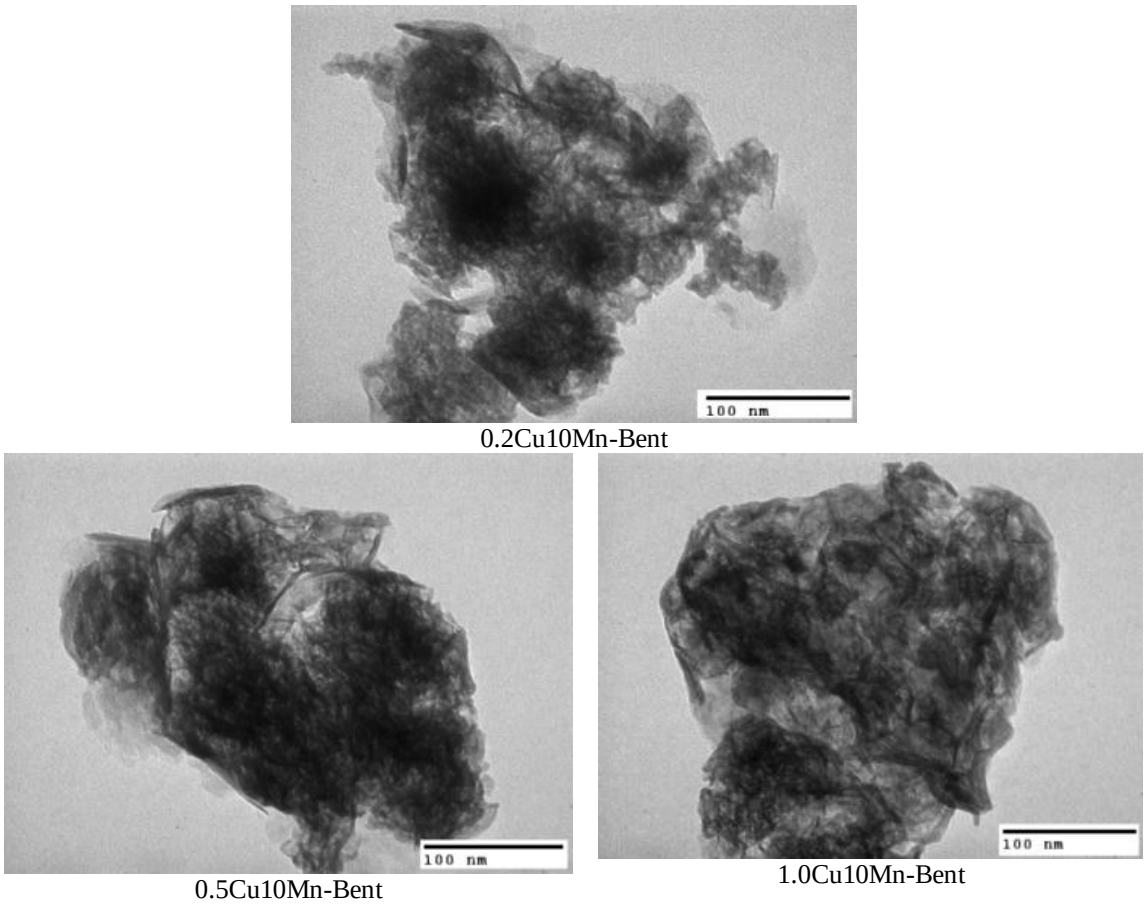

0.2Cu10Mn-Bent

0.5Cu10Mn-Bent

1.0Cu10Mn-Bent

Fig. 7: TEM images of CuMn-Bent samples.

Table-2: The elemental composition of CuMn-Bent samples.

Sample	Weight %							
	O	Si	Fe	Mn	Mg	Al	K	Cu
10Mn-Bent	44.59	14.03	13.74	9.14	3.72	2.31	1.07	0.17
0,2Cu10Mn-Bent	45.09	14.32	14.04	9.09	3.57	2.30	1.05	0.35
0,5Cu10Mn-Bent	43.66	14.59	13.83	8.99	3.68	2.29	1.11	0.68
1Cu10Mn-Bent	44.06	14.16	13.24	9.63	3.60	2.34	1.12	1.32

Catalytic activity of CuMn-Bent samples

Fig. 8 and Table-3 show TPR-H_2 profiles of 1Cu10Mn-Bent corresponding to consumed hydrogen, respectively. It is clear from the Fig. 8 those characteristic peaks of 10Mn-Bent still remains in 1.0Cu10Mn-Bent sample. However, a new peak at the temperature of 196.8 ^oC is also observed. It can be related to the reduction of CuO to Cu metal [19, 20]. In addition, there is a shoulder appearing next to each peak characteristic for MnO_x at lower temperature side. This observation can be explained by the presence of Cu in the synthesized material. The lower reduction temperatures of MnO_x can be attributed to the interaction between Cu and Mn in the material. Furthermore, the presence of Cu makes material itself become easier to be reduced with higher amount of consumed hydrogen (4.31 mmol g^{-1}, Table-3) in comparison with the sample without Cu. This result reveals that the reduction occurs on the 1.0Cu10Mn-Bent comparatively better than reduction on 10Mn-Bent.

Table-3: Consumed hydrogen of 1.0Cu10Mn-Bent at different temperatures.

Temperature of reduction peak [^oC]	*Consumed hydrogen [mmol g^{-1}]*
196.8	0.32
223.7	0.52
345.7	1.08
595.1	2.02
674.7	0.33
689.4	0.04
Total	4.31

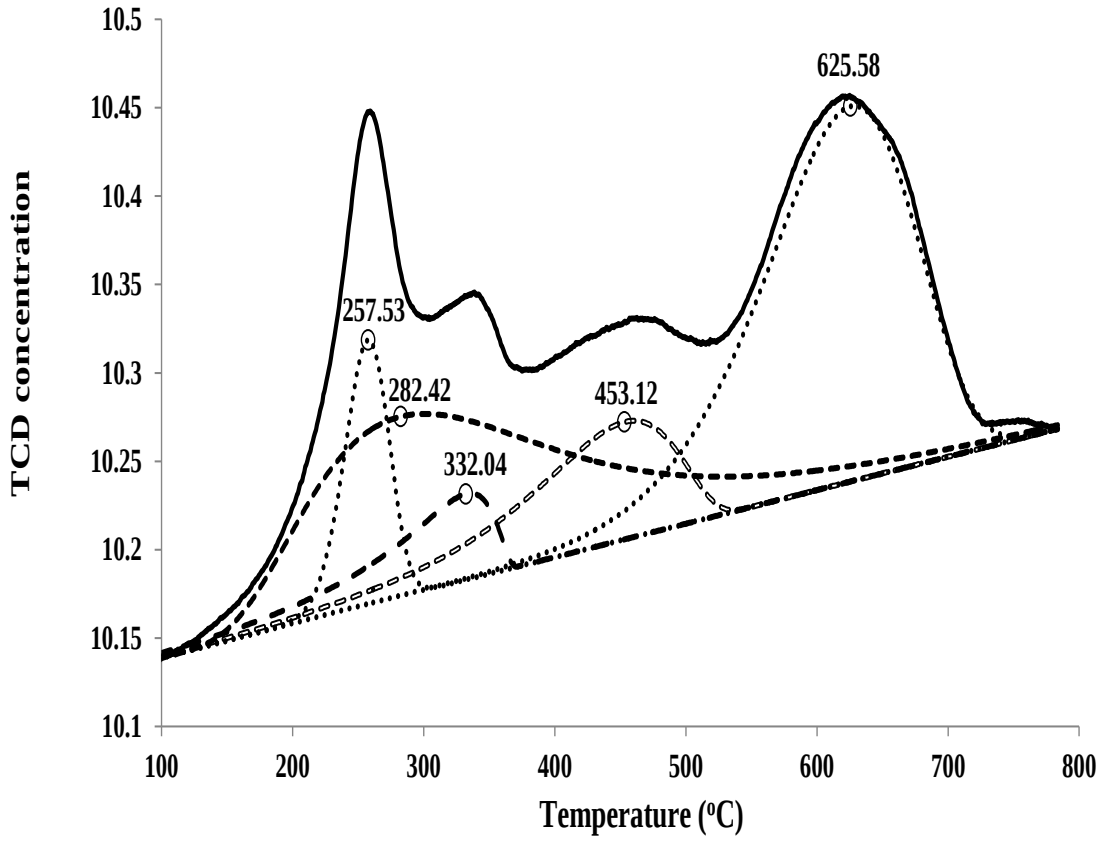

(a)

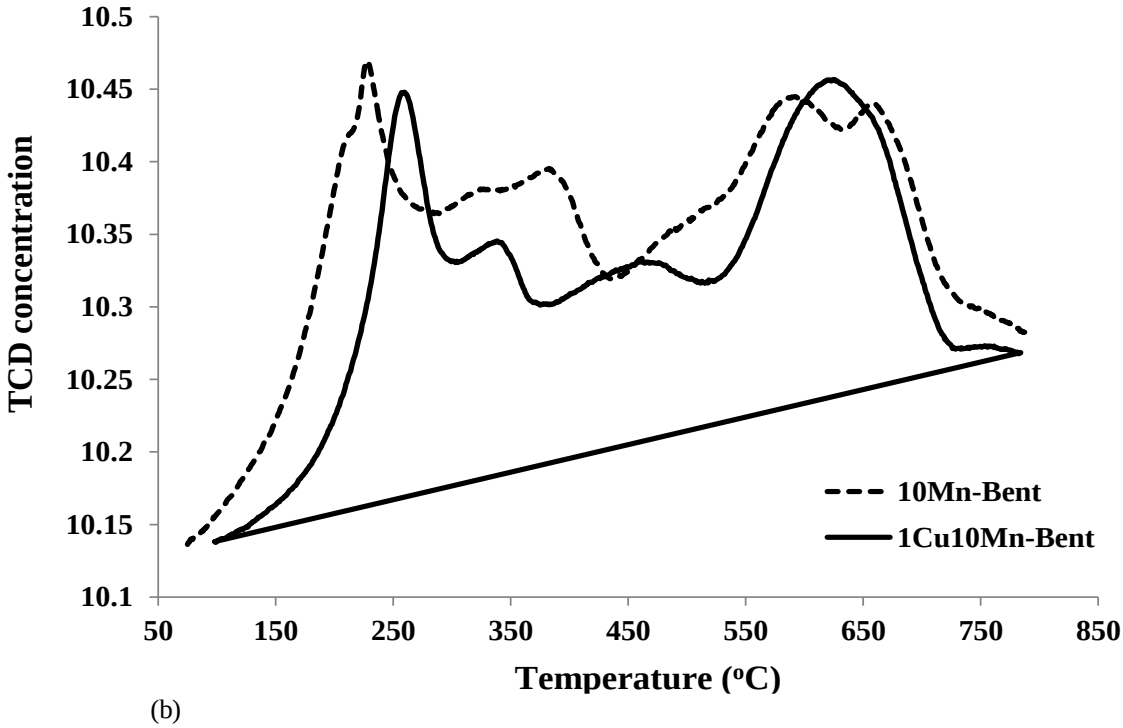

(b)

Fig. 8: TPR-H_2 profiles of 10Mn-Bent and 1.0Cu10Mn-Bent.

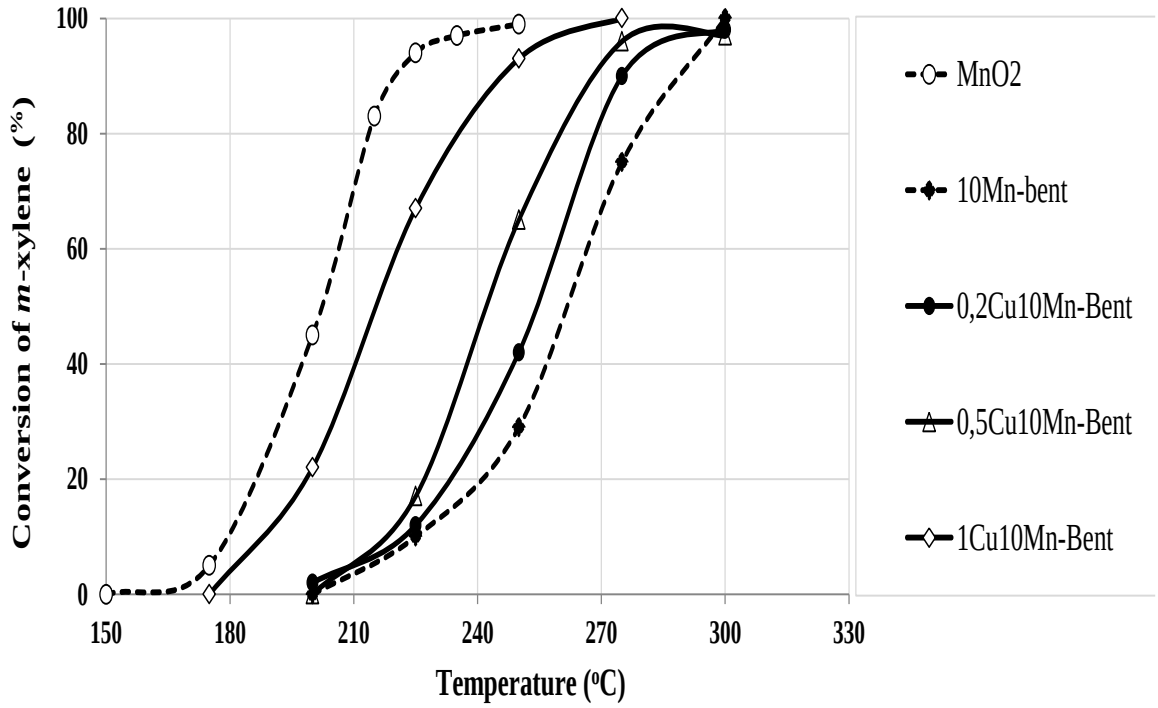

Fig. 9: Catalytic activity of CuMn –Bent on the oxidation of m-xylene.

Catalytic performance of CuMn-Bent samples on the oxidation of m-xylene

The catalytic activity results of CuMn-bent samples are presented in Fig. 9. It can be observed that the catalytic activity of materials is enhanced with the increase of Cu loading. When Cu content increases from 0.2% to 1.0%, a significant increase of the catalytic activity can be observed. In the case of 1Cu10Mn-bent, especially, the oxidation of m-xylene starts at the temperature of 180°C. The conversion reaches 50% at the temperature of 210°C and 100% at the 250°C. This result can be comparable with result obtained from MnO_2 sample though the catalyst component in 1Cu10Mn-Bent is of about 10% that of in the MnO_2 sample. This result also reveals that the combination of CuO and MnO_x has produced a good material which can oxidize m-xylene at the relatively low temperature and has a high potential application to remove VOCs present in wasted air.

Conclusion

Mn-Bent and CuMn-Bent materials with different Cu and Mn loadings were prepared for catalytic incineration of m-xylene by H_2-TPR analysis.

For Mn-Bent materials, when Mn content reaches 10% the material reveals the highest catalytic oxidation activity with the m-xylene conversion of 100% at the temperature lower than 325°C though this catalytic activity is till lower than that of pure MnO_x.

The additional introduction of Cu on the bentonite surface has improved the catalytic activity of Mn-Bent materials. At the Cu content of 1.0%, material has the highest catalytic activity compareable with the pure MnO_x sample. The presence of Cu in Mn-Bent sample also reduces the temperature of the oxidation of m-xylene, in which conversion of m-xylene reaches 100% at the temperature of 250 °C. The introduction of Cu to Mn-Bent produces a new material having a potential application on oxidizing VOCs including m-xylene present in the wasted air.

References

1. D. Rusu, Destruction of volatile organic compounds by catalytic oxidation, *Environ. Eng. Manag. J. 2(4), 273 (2003).*
2. S. C. Kim, W. G. Shim, Catalytic combustion of VOCs over a series of manganese oxide catalysts, *Appl. Catal. B-Environ. 98, 180 (2010).*

3. W. Tang, X. Wu, D. Li, Z. Wang, G. Liu, H. Liu, Y. Oxalate route for promoting activity of manganese oxide catalysts in total VOCs' oxidation: effect of calcination temperature and preparation method, *Mater. Chem.* A 2, 2544 (2014).
4. J. Luo, Q. Zhang, A. Huang, S. L. Suib, Total oxidation of volatile organic compounds with hydrophobic cryptomelane-type octahedral molecular sieves,*Microporous Mesoporous Mater*. 35-36, 209 (2000).
5. Y. Wu, Y. Lu, C. Song, Z. Ma, S. Xing, Y. Gao, A novel redox-precipitation method for the preparation of α-MnO_2 with a high surface Mn^{4+} concentration and its activity toward complete catalytic oxidation of o-xylene, *Catal. Today 201, 32 (2013).*
6. M. Ozacar, A. S. Poyraz, H. C. Genuino, C-H. Kuo, Y. Meng, S. L. Suib, Influence of silver on the catalytic properties of the cryptomelane and Ag-hollandite types manganese oxides OMS-2 in the low-temperature CO oxidation, *Appl. Catal. A-Gen. 462-463, 64 (2013).*
7. Y. Deng, W. Tang, W. Li, Y. Chen, MnO_2-nanowire@NiO-nanosheet core-shell hybrid nanostructure derived interfacial Effect for promoting catalytic oxidation activity, *Catal. Today* 308, 58 (2017).
8. L. C Wang, Y. M. Liu, M. Chen, Y. Cao, H. Y. He, K. N. Fan, MnO_2 nanorod supported gold nanoparticles with enhanced activity for solvent-free aerobic alcohol oxidation, *J. Phys. Chem. C 112, 6981 (2008).*
9. Y. Kuwahara, A. Fujibayashi, H. Uehara, K. Mori, H. Yamashita, Catalytic Combustion of Diesel Soot over Fe and Ag-doped Manganese Oxides: Role of the Heteroatom-doping in the Catalytic Performances, *Catal. Sci. Technol.*, DOI: 10.1039/C8CY00077H (2018).
10. S. C. Kim, Y-K. Park, J. W. Nah, Property of a highly active bimetallic catalyst based on a supported manganese oxide for the complete oxidation of toluene, *Powder technol. 266, 292 (2014).*
11. Y. Guo, C. Zhao, J. Lin C. Li, S. Lu, Facile synthesis of supported copper manganese oxides catalysts for low temperature CO oxidation in confined spaces, *Catal. Comm. 99, 1 (2017).*
12. S. Behar, N-A. Gómez-Mendoza, M. A. Gómez-García, D. Świerczyński, F. Quignard, N. Tanchoux, Study and modelling of kinetics of the oxidation of VOC catalyzed by nanosized Cu–Mn spinels prepared via an alginate route, *Appl. Catal. A-Gen. 504, 203 (2015).*
13. F. Wang, H. Dai, J. Deng, G. Bai, K. Ji, Y. Liu, Manganese Oxides with Rod-, Wire-, Tube-, and Flower-Like Morphologies: Highly Effective Catalysts for the Removal of Toluene, *Environ. Sci. Technol. 46, 4034 (2012).*
14. Lin, H., Chen, D., Liu, H., Zou, X., Chen, T., Effect of MnO_2 Crystalline Structure on the Catalytic Oxidation of Formaldehyde, *Aerosol Air Qual. Res. 17, 1011–1020 (* 2017).
15. X. Wang, Y. Li, synthesis and formation mechanism of manganese dioxide nanowires/nanorods, *Chem. Eur. J. 9 (1), 300 (2003).*
16. L. Kang, m. Zhang, Z-H. Liu, K. Ooi K, IR spectra of manganese oxides with either layered or tunnel structures, *Spectrochim. Acta A 67, 864 (2007).*
17. S. Liang, F. Teng, G. Bulgan, R. Zong, Y. Zhu, Effect of phase structure of MnO_2 nanorod catalyst on the activity for CO oxidation, *J. Phys. Chem. C* 112, *5307 (2008).*
18. J. E. Colman-Lerner, M. A. Peluso, J. E. Sambeth, H. J. Thomas, Catalytic removal of a mixture of volatile organic compounds present in indoor air at various work sites over Pt, MnO_x and Pt/MnO_x supported monoliths, *Reac. Kinet. Mech. Cat. 108, 443 (2013).*
19. T. Tabakova, F. Boccuzzi, M. Manzoli, J. Sobczak, V. Idakiev, D. Andreeva, A comparative study of nanosized IB/ceria catalysts for low-temperature water-gas shift reaction, *Appl. Catal. A-Gen. 298, 127 (2006).*
20. D. Delimaris, T. Ioannides, Appl. VOC oxidation over CuO–CeO_2 catalysts prepared by a combustion method, *Catal. B-Environ.* 89, 295 (2009).